Hair-bundle movements elicited by transepithelial electrical stimulation of hair cells in the sacculus of the bullfrog

D. Bozovic and A. J. Hudspeth*

The Howard Hughes Medical Institute and Laboratory of Sensory Neuroscience, The Rockefeller University, 1230 York Avenue, New York, NY 10021

Electrically evoked otoacoustic emission is a manifestation of reverse transduction by the inner ear. We present evidence for a single-cell correlate of this phenomenon, hair-bundle movement driven by transepithelial electrical stimulation of the frog's sacculus. Responses could be observed at stimulus frequencies up to 1 kHz, an order of magnitude higher than the organ's natural range of sensitivity to acceleration or sound. Measurements at high-stimulus frequencies and pharmacological treatments allow us to distinguish two mechanisms that mediate the electrical responses: myosin-based adaptation and Ca^{2+}-dependent reclosure of transduction channels. These mechanisms also participate in the active process that amplifies and tunes the mechanical responses of this receptor organ. Transient application of the channel blocker gentamicin demonstrated the crucial role of mechanoelectrical transduction channels in the rapid responses to electrical stimulation. A model for electrically driven bundle motion that incorporates the negative stiffness of the hair bundle as well as its two mechanisms of motility captures the essential features of the measured responses.

T he inner ear uses a mechanical amplifier to boost the sensitivity and acuity of hearing. When an acoustic stimulus vibrates the elastic basilar membrane of the mammalian cochlea, for example, outer hair cells in the organ of Corti are excited. These cells in turn exert forces that augment basilar-membrane motion, thus partly overcoming the effect of viscous damping imposed by the fluids of the inner ear. The cochlear active process displays four characteristics: mechanical amplification, frequency discrimination, nonlinearity, and the production of otoacoustic emissions (reviewed in refs. 1 and 2).

Electrical as well as acoustic stimulation can excite the cochlea. Passing sinusoidal current across the cochlear partition elicits the emission from the ear of sound at the frequency of stimulation (3). When electrical stimulation is applied, the basilar membrane is driven into oscillation; the resultant pressure change oscillates the bones of the middle ear and emerges as a sound, an electrically evoked otoacoustic emission (EEOAE).

The active process of the mammalian cochlea is thought to be membrane-based electromotility, that is, voltage-driven alteration in the somatic length of outer hair cells (reviewed in refs. 4 and 5). The lateral plasmalemma of an outer hair cell contains $\approx 10^7$ molecules of prestin (6), a protein that responds to changes in membrane potential by rapid structural rearrangement. Although the mechanical coupling of cellular motion to basilar-membrane movement remains unclear, the cyclic changes in cellular length during sinusoidal electrical stimulation are thought to pump energy into the basilar membrane's oscillation. In support of the role of prestin in the active process, disruption of the prestin gene significantly elevates the threshold of hearing (7).

It is plausible that electrical stimulation directly activates prestin molecules, producing cellular length changes that account for EEOAEs. Nevertheless, the connection between electromotility and emissions remains uncertain. Certain properties

of EEOAEs from the mammalian ear suggest that the mechanical response is associated with the gating of transduction channels (ref. 8; but see ref. 9). Moreover, electrical stimulation elicits otoacoustic emissions from the cochleae of a lizard, the bobtail skink, and a bird, the chicken (10–12). Because the ears of nonmammalian tetrapods lack outer hair cells, and inasmuch as their hair cells have not been reported to contain prestin or to exhibit high-frequency electromotility, this observation implies that the inner ear contains an additional voltage-sensitive mechanical element. The temporal structure of the lizard's emissions implicates hair bundles, the mechanoreceptive organelles of hair cells, as their source (12). This result therefore adds to the evidence that active hair-bundle motility constitutes the active process, at least in the ears of nonmammalian tetrapods (reviewed in refs. 13–15). Bundle motility displays all four hallmarks of the aural active process. Hair bundles can amplify mechanical stimuli (16, 17) and enhance the frequency selectivity of responsiveness (17). Bundles display nonlinearities that resemble those measured in the intact cochlea (17, 18). Finally, unstimulated hair bundles produce oscillations that may underlie spontaneous otoacoustic emissions (refs. 16 and 19 and P. Martin, D.B., Y. Choe, and A.J.H., unpublished data).

Because hair bundles mediate mechanoelectrical transduction in all hair cells, including those of the mammalian cochlea, their possible electrical sensitivity might be a characteristic of the active process of acousticolateralis sensory organs in general. It is therefore important to confirm the existence of electrically evoked bundle motility and to understand its mechanism. In the present study, we have tested directly the inference that electrical stimulation drives hair-bundle movements and used modeling to examine the mechanisms that underlie the observed responses.

Materials and Methods

Experimental Preparation. Saccular maculae were dissected from the internal ears of adult bullfrogs (*Rana catesbeiana*) into oxygenated standard saline solution comprising 110 mM of Na^+, 2 mM K^+, 4 mM Ca^{2+}, 118 mM Cl^-, 3 mM D-glucose, and 5 mM Hepes. Each macula was mounted in a two-compartment experimental chamber that mimicked physiological conditions by exposing the apical and basal surfaces to dissimilar solutions (16). The basal compartment was filled with standard saline solution and the apical compartment with artificial endolymph consisting of 2 mM Na^+, 118 mM K^+, 0.25 mM Ca^{2+}, 118 mM Cl^-, 3 mM D-glucose, and 5 mM Hepes. Both solutions were oxygenated immediately before use. To facilitate the removal of the otolithic membrane, we digested each macula for 20–30 min at room temperature in 50 μg·ml^{-1} of protease (type XXIV, Sigma).

Electrical Stimulation. Transepithelial electrical currents were applied with a stimulus isolation unit (A395, World Precision

---

Abbreviation: EEOAE, electrically evoked otoacoustic emission.

*To whom correspondence should be addressed. E-mail: hudspaj@rockefeller.edu.

Instruments, Sarasota, FL), a constant-current source with an isolated ground. Agar-filled glass electrodes in contact with chlorided silver wires were used to pass stimulus current between the two compartments of the experimental chamber. Each hair cell lies in parallel with the comparatively low and constant resistance of 30–50 kΩ afforded by the saccular epithelium. A constant current therefore produces a fixed transepithelial voltage drop that is divided between the apical and basolateral membrane surfaces of each hair cell in proportion to their respective impedances (21).

Transepithelial stimulation polarizes the apical and basolateral membrane surfaces of a hair cell in opposite senses. The ionic current relevant to hair-bundle motility is that across the apical membrane, which includes the membrane of the stereocilia and the kinocilium of each hair bundle. We define a positive stimulus as that causing the flow of conventional current from the basolateral to the apical compartment of the experimental chamber. Current of this polarity, which depolarizes the apical membrane surface, is displayed as a positive deflection in all figures.

Measurement of Hair-Bundle Movement. The techniques for mechanical stimulation, imaging, and optical calibration have been described in detail (refs. 16, 22, and 23 and P. Martin, D.B., Y. Choe, and A.J.H., unpublished data). The saccular epithelium was imaged in an upright microscope and illuminated with a mercury lamp whose light was passed through a heat filter and a band-pass filter of 500 ± 40 nm (center wavelength $\pm$ range to half transmittance). Individual hair bundles were imaged through a $\times 40$ water-immersion lens of numerical aperture 0.8. To detect the motion of a hair bundle, the tip of a sputter-coated glass fiber ≈ 100 μm in length and ≈ 0.5 μm in diameter was attached to the kinociliary bulb of the hair cell. The fiber had a stiffness of 40–250 μN·m^{-1} and a drag coefficient of 40–150 nN·s·m^{-1}. The image of the tip of the fiber was magnified 1,000 times and projected onto a dual photodiode. To calibrate the measurements of hair-bundle displacement with nanometer precision, we delivered a 20-μm offset pulse to the photodiode system immediately before each recording.

The output of the photodiode was low-pass-filtered at 2–5 kHz with an eight-pole Bessel filter and digitally sampled at 5–50 kHz; signals were recorded with LABVIEW 5.0 (National Instruments, Austin, TX). Data were analyzed and numerical modeling was conducted with MATHEMATICA 4.1.5 (Wolfram Research, Champaign, IL).

Application of Pharmacological Agents. Iontophoresis of gentamicin was accomplished with a bent glass microelectrode filled with 500 mM of drug solution. While a continuous holding current of -0.2 nA was applied, the tip of the electrode was positioned 2–5 μm above the hair bundle with a Huxley-type micromanipulator. Pulses of 3–10 nA were then used to eject gentamicin into the solution. Assuming a diffusion coefficient of 400 μm^2·s^{-1} for gentamicin and a value of 0.013 for the ratio of the drug's transference number to its valence (24), we used the diffusion equation to estimate the concentration of gentamicin at the top of the bundle. Even for a 3-nA current from an electrode 5 μm above the bundle, the steady-state concentration reached ≈ 16 μM, a level sufficient to block most of the transduction channels (24, 25).

Butanedione monoxime was prepared at a concentration of 20 mM in artificial endolymph. After measurements in artificial endolymph had been concluded, the solution in the upper compartment of the experimental chamber was replaced with butanedione monoxime solution, with repeated exchanges performed to ensure complete replacement.

Results

When exposed to solutions that mimic the natural environment of the internal ear, hair bundles of the anuran sacculus often produce spontaneous oscillations (refs. 16, 17, 22, and 26 and P. Martin, D.B., Y. Choe, and A.J.H., unpublished data). These bundle movements may exceed 100 nm in peak-to-peak magnitude and are roughly symmetrical in the positive and negative directions: each phase of motion commences with a rapid stroke and concludes with a slow movement in the same direction. Because these oscillations cannot be explained by thermal noise (19), a spontaneously active hair bundle must possess an energy source that enhances its motion. Applying a mechanical stimulus smaller than ± 1 pN to an active bundle entrains the spontaneous movements of the cell, yielding a mechanical output with power that exceeds that of the input (16, 17).

To learn whether active hair-bundle motility might also be associated with the phenomenon of EEOAE, we stimulated hair cells with transepithelial current. Movements of an individual hair bundle were measured by imaging the tip of a fine glass fiber attached near the bundle's top. When the fiber extended freely into the recording chamber or when it was attached to an inert hair bundle, the passage of stimulus current evoked little or no fiber movement. When the fiber was attached to an oscillatory hair bundle, however, sinusoidal electrical stimulation at frequencies of 1–1,000 Hz and amplitudes of 3–50 μA strongly modified the spontaneous bundle movements. The detailed nature of the response to electrical excitation depended on the stimulus frequency.

Stimulation at 1 Hz produced highly asymmetrical responses. During the negative phase of electrical excitation, which hyperpolarized the apical plasmalemma, hair-bundle oscillations increased in frequency and declined in magnitude (Fig. 1). Each cycle of movement was accelerated through omission of the slow positive component and reduction in the magnitude of motion. Positive stimulation, which corresponded to depolarization of the apical membrane, almost entirely suppressed oscillation, leaving the bundle offset in the positive direction. During this arrest, the peak of the sinusoidal stimulus was associated with slight movement of the bundle in the negative direction.

At frequencies significantly below a bundle's frequency of spontaneous oscillation, or natural frequency, electrical stimulation produced similar modulatory effects on bundle movement (Fig. 1). One or more small, fast strokes occurred during each negative phase of a stimulus cycle; during each positive phase, oscillation was suppressed and the bundle deflected in the positive direction. Throughout this frequency range, the slow oscillatory component of the mechanical response was therefore in phase with the electrical stimulus.

Electrical stimulation elicited entrained mechanical responses at high frequencies, usually up to 300–500 Hz (Fig. 1); small oscillations could occasionally be evoked by 1-kHz excitation (data not shown). To produce consistent responses at these frequencies, it was usually necessary to increase the amplitude of stimulation from 10 to 30 μA. For stimulus frequencies near 100 Hz, the response polarity was opposite that observed for low-frequency stimulation: the negative phase of electrical stimulation induced a positive bundle movement, and the positive phase a negative motion. As the frequency increased further, the mechanical response, in addition to being inverted with respect to the stimulus, displayed the time delay expected from the low-pass filtering properties of the glass fiber, whose average stiffness and drag coefficient implied a time constant of up to ≈ 1 ms. During stimulation at a few hundred hertz, slow bundle oscillations near the natural frequency were often superimposed on the fast, phase-locked responses. Electrical stimulation at these high frequencies decoupled two components of bundle motility owing to their different time scales of responsiveness.
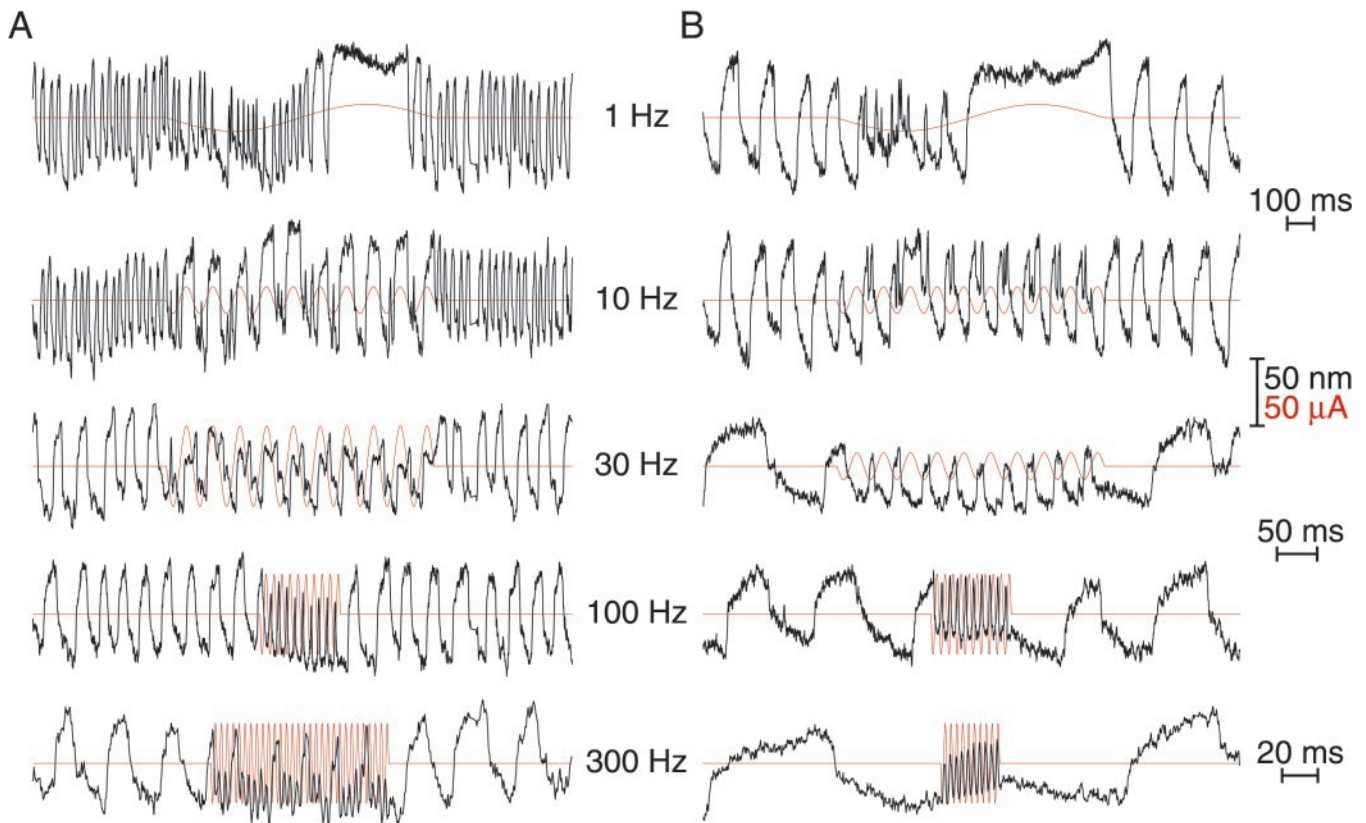
Fig. 1. Response of active hair bundles to stimulation by sinusoidal transepithelial current. (*A*) Before stimulation, a hair bundle oscillated spontaneously at ≈35 Hz. During negative stimulation at 1 Hz, the bundle displayed faster and smaller oscillations with occasional omissions; the positive stimulus phase slowed and eventually blocked oscillatory movements. Similar responses occurred during stimulation at 10 Hz. At 30 Hz, slightly below the natural frequency of the cell, the response comprised phase-locked movements adorned with complex spikes. At 100 and 300 Hz, the response was essentially out of phase with the stimulus. During a 300-Hz stimulation, spontaneous bundle oscillations resumed, superimposed on the rapid, phase-locked response. (*B*) The hair bundle of a second cell oscillated spontaneously at ≈8 Hz. Although electrical stimulation evoked responses similar to those in *A*, the transition from the low- to the intermediate-frequency regime of responsiveness occurred at a frequency <10 Hz. In this and the subsequent figures, each mechanical response is superimposed on a record of the electrical stimulus (red). Positive bundle movement is defined as that towards the kinocilium. Positive current is defined as that depolarizing the apical membrane of the hair cell. The top time calibration applies to the 1- and 10-Hz records, the middle calibration corresponds to the 30- and 100-Hz records, and the bottom calibration refers only to the 300-Hz records.

In the intermediate frequency range near a bundle's natural frequency, the complex response to electrical stimulation reflected the interaction of the two behaviors described previously (Fig. 1). The low-frequency response component continued to be entrained at the stimulus frequency. At the same time, faster twitches appeared during either phase of stimulation.

To emphasize the repeatability of the entrained bundle movements at moderate to high frequencies of stimulation, we averaged responses to repeated bursts of sinusoidal electrical current. Because of their variable phase and frequency, spontaneous oscillations were averaged-out in these recordings. This procedure confirmed that the response was rapid and of a polarity opposite that of the stimulus (Fig. 2*A*). After the cessation of stimulation, the bundle exhibited a damped, sinusoidal oscillation at a frequency near that of its spontaneous oscillation.

To observe more clearly the dynamics and polarity of the response, we applied single, 1-ms pulses of electrical stimulation. The resulting impulse response was large, up to ≈100 nm, and rapid, lagging the stimulus by <1 ms (Fig. 2*B*). Because this measurement was limited by the filtering properties of measurement system, it represents an upper limit on the response latency. The polarity of the response was opposite that of the stimulus. The response was nonlinear, for the negative pulse evoked a much larger movement

than did the positive one. The averaged response again demonstrated damped oscillations after stimulation.

A hair bundle's oscillation in the absence of stimulation can largely be explained by the activity of myosin-based adaptation motors (ref. 23 and P. Martin, D.B., Y. Choe, and A.J.H., unpublished data). To examine the role of these motors in electrically driven hair-bundle movements, we applied butanedione monoxime, a drug that interferes with the ATPase cycle of myosin by promoting weak binding to actin filaments (27). As reported (P. Martin, D.B., Y. Choe, and A.J.H., unpublished data), butanedione monoxime completely suppressed spontaneous oscillations (Fig. 3*A*). Electrically driven hair-bundle motion, however, remained intact and sometimes increased in magnitude.

To test the role of transduction-channel gating in electrically driven hair-bundle motion, we blocked the channels with gentamicin. This aminoglycoside antibiotic, which rapidly and reversibly blocks transduction channels in the open state (28, 29), arrests spontaneous hair-bundle oscillation (P. Martin, D.B., Y. Choe, and A.J.H., unpublished data). After a short delay consistent with the drug's diffusion from an iontophoretic pipette, gentamicin largely suppressed electrically evoked bundle movement (Fig. 3*B*). As expected for the open-channel-blocking action of the drug, the motion was arrested with the bundle deflected in the positive direction. The process was
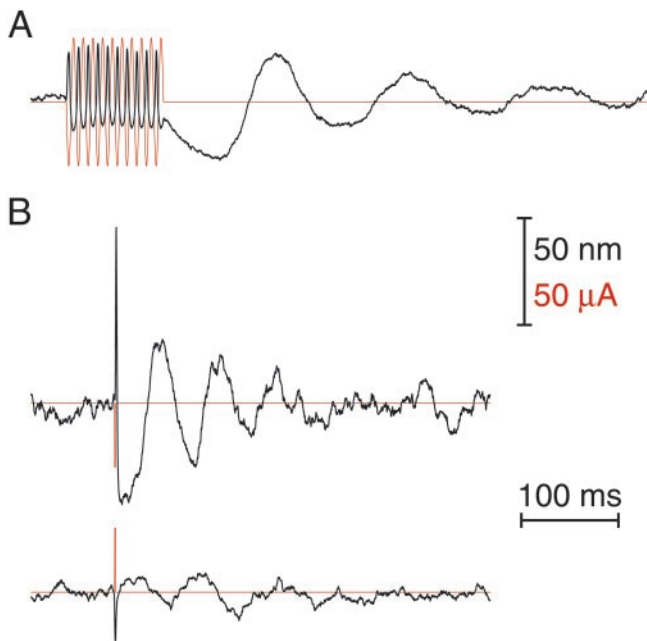
Fig. 2. Time scales of hair-bundle responsiveness to electrical stimulation. (*A*) Application of 10 cycles of 100-Hz electrical current entrained the motion of the bundle, eliciting movements of a polarity opposite that of the stimulus. After cessation of the stimulus, a damped oscillation occurred at the cell's natural frequency of ≈7 Hz. (*B*) Electrical pulses 1 ms in duration elicited rapid mechanical responses of opposite polarity, followed by a slower oscillation at the natural frequency of the cell of ≈16 Hz. Note the asymmetry in the responses to negative (*Upper*) and positive (*Lower*) stimuli. Each of the three records displays the average of 50 successive measurements.

reversible: at the conclusion of gentamicin iontophoresis, the electrically driven oscillations quickly recovered. This result suggests that electrically evoked hair-bundle movements stem from modulation of the current through transduction channels rather than a direct effect of voltage.

Discussion

When mechanically stimulated, hair bundles produce responses on two distinct time scales. The application of a force step to a bundle produces a rapid elastic deflection that is followed by a gradual relaxation associated with adaptation of the mechano-electrical transduction process (22, 26, 30–34). Extensive evidence indicates that this mechanical response, which transpires with a time constant of 10–300 ms, is mediated by myosin-based adaptation motors (reviewed in refs. 35–37). Mechanical stimulation also evokes a swifter bundle movement that may be oscillatory (33, 34, 38, 39) or transient (22, 26, 30). Ca^{2+}-dependent reclosure of transduction channels underlies this rapid response, which occurs in a few milliseconds (reviewed in refs. 13 and 15).

A hair bundle responds to electrical stimulation in two distinct ways. On a time scale of tens to hundreds of milliseconds, depolarization through an intracellular electrode yields a negatively directed bundle movement (34, 40–45). This response reflects a depolarization-induced decrease in Ca^{2+} entry into stereocilia and the consequent enhancement of climbing adaptation by the myosin-based motors. On a shorter time scale of a few milliseconds, depolarization elicits positive bundle motion (34, 38, 39, 43). This movement signifies a reduction in Ca^{2+}-dependent channel reclosure as depolarization stems the influx of Ca^{2+}. By electrically stimulating hair cells over a broad range of frequencies with transepithelial current, we have garnered
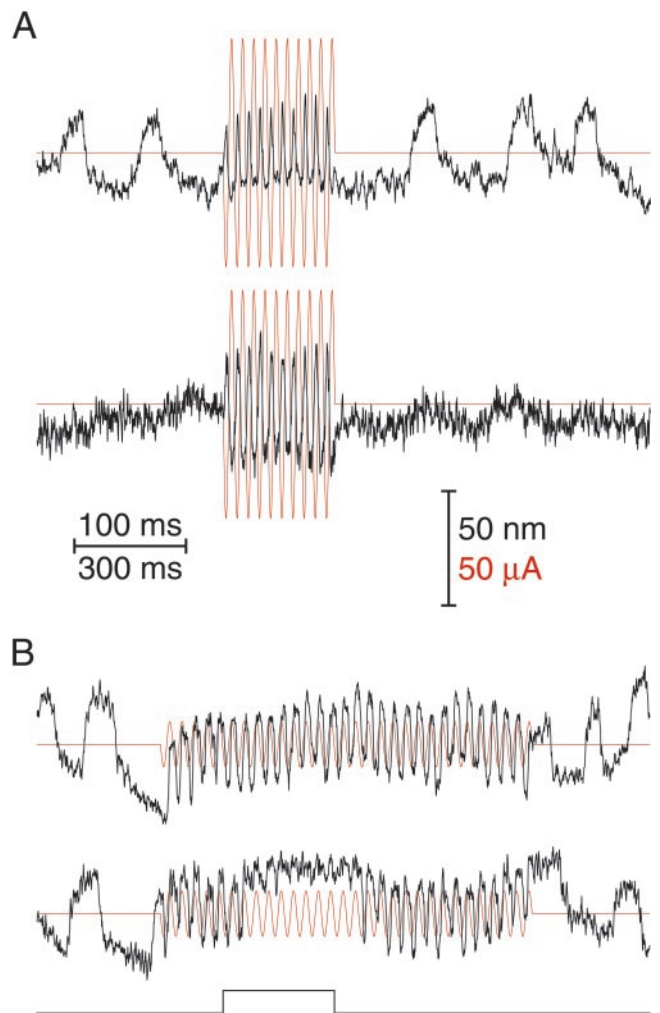
Fig. 3. Effects of butanedione monoxime and gentamicin on electrically evoked hair-bundle movements. (*A*) Under control conditions, a hair bundle oscillated spontaneously and responded to electrical stimulation at 100 Hz (*Upper*). In the presence of 20 mM butanedione monoxime, the same bundle produced a comparable electrical response without spontaneous oscillation (*Lower*). The high-frequency spikes of bundle motion in the latter record might reflect the residual activity of myosin molecules. (*B*) A spontaneously active hair bundle responded well under control conditions to 30-Hz electrical stimulation (*Upper*). The electrical response was blocked when the same bundle was exposed to gentamicin (*Lower*), whose iontophoretic application is indicated beneath the recording. Drug exposure offset the bundle in the positive direction, an indication of blockage in the open-channel state.

additional information about the mechanisms underlying the active process in hair bundles of the frog's sacculus.

Duality of Force-Producing Mechanisms. The present experiments provide three lines of evidence in support of the inference that there are two force-producing mechanisms that interact to provide the active process of hair cells. First, during stimulation at frequencies of a few hundred hertz, hair-bundle motion frequently resolved into two largely independent but superimposed components. Limit-cycle oscillations continued at a frequency and magnitude similar to those in the unstimulated bundle; the activity of adaptation motors can explain these low-frequency movements (ref. 17 and P. Martin, D.B., Y. Choe, and A.J.H., unpublished data). The acceleration of these oscillations during electrical stimulation probably reflected the accumulation of Ca^{2+} in the stereociliary cytoplasm (11). A second

BIOPHYSICS

component of bundle movement followed the electrical stimulus on a cycle-by-cycle basis. This response likely originated from Ca^{2+}-dependent channel reclosure, a process that can operate at high frequency (refs. 30 and 46; reviewed in ref. 15).

Pharmacological sensitivity provides a second line of evidence for two force-producing mechanisms. By interfering with myosin-based motility and hence inhibiting adaptation, butanedione monoxime abolished spontaneous hair-bundle movement. Under the same conditions, however, high-frequency responsiveness to electrical stimulation, a process driven by Ca^{2+}-dependent channel reclosure, persisted with little or no attenuation. Butanedione monoxime similarly spares the rapid component of a bundle's response to mechanical stimulation (33).

By demonstrating two time scales of responsiveness, the hair bundle's impulse response provides the third argument for two mechanisms. Brief stimuli of either polarity evoked a transient only a few milliseconds in length. This fast response was succeeded by a damped sinusoidal oscillation on a much slower time scale. The brevity of the former movement implicates channel reclosure in its genesis; the sensitivity of the latter to butanedione monoxime implies that it stems from myosin-based adaptation.

A Model for Electrically Evoked Hair-Bundle Movements. Although the waveforms of the hair-bundle movements evoked by sinusoidal electrical stimulation are complex, their essential features accord with the results of a model for active hair-bundle motility that subsumes three essential components (P. Martin, D.B., Y. Choe, and A.J.H., unpublished data). First, an active hair bundle displays negative stiffness over a specific range of displacements (23). This property emerges from gating compliance, the reduction in bundle stiffness resulting from the opening and closing of transduction channels (ref. 30; reviewed in refs. 14 and 47). The second constituent of the model is the ensemble of myosin-based motors that mediates the adaptation process of the hair cell (reviewed in refs. 35–37). Adaptation serves as a tuning mechanism that strives to situate the hair bundle in its range of negative stiffness. Because the bundle cannot reside stably within this region, it undergoes a spontaneous oscillation (ref. 19 and P. Martin, D.B., Y. Choe, and A.J.H., unpublished data). The final component of the model is a Ca^{2+}-driven mechanism for reclosure of mechanoelectrical-transduction channels (30, 33, 34, 39, 48, 49). As the channels close, the tension in each associated gating spring increases, pulling the hair bundle in the negative direction. This process underlies active hair-bundle motility that can both foster spontaneous bundle oscillation and amplify mechanical inputs (33, 46).

Ca^{2+} affects all three of the proposed components of active hair-bundle motility in ways that have been incorporated into the model (P. Martin, D.B., Y. Choe, and A.J.H., unpublished data). First, extracellular Ca^{2+} regulates hair-bundle stiffness (34, 50); at the low concentration characteristic of the natural environment of the bundle, this stiffness can become negative (23). Second, Ca^{2+} controls the activity of adaptation motors (51, 52). Probably by binding to calmodulin (53, 54) associated with myosin Ic (55, 56), Ca^{2+} increases the propensity of each motor to slip down a stereocilium in response to gating-spring tension (42). Third, Ca^{2+} promotes reclosure of the transduction channel. To explain the present and earlier results, we have supposed in the present model that Ca^{2+} entering through a transduction channel does not directly shut it but rather binds to an elastic reclosure element associated with the channel. Binding decreases the stiffness of this element, allowing the hair bundle to move in the positive direction. The reduced tension in the gating spring subsequently permits the channel to close, pulling the bundle in the negative direction (P. Martin, D.B., Y. Choe, and A.J.H., unpublished data). In support of this formulation, the response to a negative current pulse displayed a biphasic character: the initial stroke in the positive direction was followed by
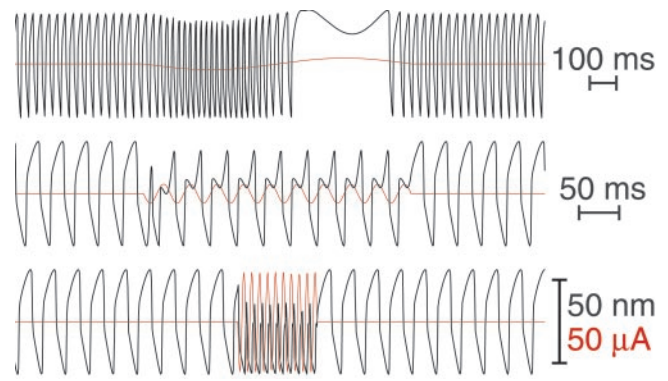
Fig. 4. Modeling of electrically evoked hair-bundle movements. Stimulation at 1 Hz (*Top*) accelerated bundle oscillation during the negative phase of stimulation and arrested movement during the positive phase. Excitation with a 30-Hz current (*Middle*) mimicked the intermediate regime of bundle responsiveness, with complex but phase-locked bundle movements. The modeled response to 100-Hz stimulation (*Bottom*) displays phase-locking, with movements of a polarity opposite that of stimulation. The three records correspond to those for the same stimulus frequencies in Fig. 1*A*. Except for the frequency and amplitude of stimulation, the values of all parameters in the model were identical in the three simulations. The uppermost time calibration refers to the top record and the second calibration to both subsequent records; the distance and current calibrations apply to all three records.

motion in the negative direction before the onset of slower oscillation. Moreover, in the presence of butanedione monoxime, the positive transient response to a negative stimulus pulse was followed by a short movement in the opposite direction (data not shown). The hypothetical Ca^{2+}-binding site and relaxation element remain unidentified. Because each transduction channel is thought to be connected to actin filaments through an array of myosin Ic molecules (reviewed in refs. 35 and 36), the binding site might be one or more of the associated calmodulin molecules (53, 54). Ca^{2+} binding to myosin-bound calmodulin could induce a conformational change that renders the neck region of myosin more compliant (36, 57). Alternatively, Ca^{2+} binding might cause some myosin molecules to dissociate from actin, leaving fewer to contribute to the rigidity of the connection.

The behavior of hair bundles during low-frequency stimulation may be understood in terms of the effect of voltage on Ca^{2+} entry into the stereociliary cytoplasm (Fig. 4). By hyperpolarizing the apical plasmalemma, negative stimulation increases the driving force on Ca^{2+} and therefore augments the ion's influx. An increased stereociliary Ca^{2+} concentration facilitates rapid channel reclosure, leading to smaller, faster oscillations. A similar effect occurs when the extracellular Ca^{2+} concentration is raised by iontophoretic application of Ca^{2+} to a hair bundle (P. Martin, D.B., Y. Choe, and A.J.H., unpublished data). Conversely, positive current reduces the influx of Ca^{2+} with two consequences, the first mediated by Ca^{2+}-dependent channel reclosure and the second by adaptation. A reduction of the stereociliary Ca^{2+} concentration diminishes channel reclosure and hence allows the bundle to move in the positive direction. When the Ca^{2+} concentration becomes still smaller, however, the enhanced climbing activity of the adaptation motor begins to pull the bundle back in the negative direction. The latter effect has been observed during depolarization of a hair cell through a tight-seal electrode (42).

For the high-frequency regime of responsiveness, the model confirms that electrical stimulation produces rapid, phase-locked bundle movements driven by Ca^{2+}-dependent reclosure of transduction channels. The response polarity results from the

effect of the hypothetical relaxation element, for negative stimulation, which should promote Ca^{2+} entry into the stereociliary cytoplasm, produces a positive bundle movement. A similar rationale explains the polarity of the fast component of the impulse response.

Finally, the response of a hair bundle to electrical stimulation near its natural frequency is more complex. In this intermediate regime of responsiveness, the myosin-based component of the bundle's movement follows the stimulus on a one-to-one basis. The response waveform is highly irregular, however, owing to the presence of rapid movements produced by channel reclosure. The model captures much of the intricacy of this response (Fig. 4).

Relationship of Responses to Cochlear Emissions. The present experiments demonstrate that an individual hair bundle can produce vigorous oscillations during sinusoidal electrical stimulation. We believe this response to be a single-cell correlate of EEOAE. When an electrical stimulus entrains bundle motion, an ensemble of hair cells exposed to the same stimulus and coupled through an accessory structure (a tectorial membrane or sallet) would be expected to oscillate in unison. Operating through the micromechanical linkages of the receptor organ, such a group of oscillating hair bundles would drive basilar-membrane motion. The resultant changes in the pressure between the scala media and scala tympani would then be manifested as an otoacoustic emission.

It is striking that electrically evoked hair-bundle movements can be detected in anuran hair cells at frequencies tenfold as great as the upper extreme of normal saccular sensitivity (20). Moreover, because of the filtering properties of the measurement system, the observed bundle movements represent the lower limit of actual cellular responsiveness. An active process based on hair-bundle motility therefore seems fast enough to potentially operate in other organisms, such as reptiles and birds, whose range of hearing and otoacoustic emission extends to ≈ 10 kHz. Whether the same process can encompass the higher-frequency responses of the mammalian ear remains unknown.

1. Manley, G. (2000) *Proc. Natl. Acad. Sci. USA* **97,** 11736–11743.
2. Manley, G. A. (2001) *J. Neurophysiol.* **86,** 541–549.
3. Hubbard, A. E. & Mountain, D. C. (1983) *Science* **222,** 510–512.
4. Dallos, P. (1992) *J. Neurosci.* **12,** 4575–4585.
5. Nobili, R., Mammano, F. & Ashmore, J. (1998) *Trends Neurosci.* **21,** 159–167.
6. Zheng, J., Shen, W., He, D. Z. Z., Long, K. B., Madison, L. D. & Dallos, P. (2000) *Nature* **405,** 149–155.
7. Liberman, M. C., Gao, J., He, D. Z. Z., Wu, X., Jia, S. & Zuo, J. (2002) *Nature* **419,** 300–304.
8. Yates, G. K. & Kirk, D. L. (1998) *J. Neurosci.* **18,** 1996–2003.
9. Kirk, D. L. (2001) *Hear. Res.* **161,** 99–112.
10. Chen, L., Sun, W. & Salvi, R. J. (2001) *Hear. Res.* **161,** 54–64.
11. Manley, G. A. & Kirk, D. L. (2001) *J. Assoc. Res. Otolaryngol.* **3,** 200–208.
12. Manley, G. A., Kirk, D. L., Köppl, C. & Yates, G. K. (2001) *Proc. Natl. Acad. Sci. USA* **98,** 2826–2831.
13. Hudspeth, A. J. (1997) *Curr. Opin. Neurobiol.* **7,** 480–486.
14. Hudspeth, A. J., Choe, Y., Mehta, A. D. & Martin, P. (2000) *Proc. Natl. Acad. Sci. USA* **97,** 11765–11772.
15. Fettiplace, R., Ricci, A. J. & Hackney, C. M. (2001) *Trends Neurosci.* **24,** 169–175.
16. Martin, P. & Hudspeth, A. J. (1999) *Proc. Natl. Acad. Sci. USA* **96,** 14306–14311.
17. Martin, P. & Hudspeth, A. J. (2001) *Proc. Natl. Acad. Sci. USA* **98,** 14386–14391.
18. Jaramillo, F., Markin, V. S. & Hudspeth, A. J. (1993) *Nature* **364,** 527–529.
19. Martin, P., Hudspeth, A. J. & Jülicher, F. (2001) *Proc. Natl. Acad. Sci. USA* **98,** 14380–14385.
20. Koyama, H., Lewis, E. R., Leverenz, E. L. & Baird, R. A. (1982) *Brain Res.* **250,** 168–172.
21. Corey, D. P. & Hudspeth, A. J. (1983) *J. Neurosci.* **3,** 942–961.
22. Benser, M. E., Marquis, R. E. & Hudspeth, A. J. (1996) *J. Neurosci.* **16,** 5629–5643.
23. Martin, P., Mehta, A. D. & Hudspeth, A. J. (2000) *Proc. Natl. Acad. Sci. USA* **97,** 12026–12031.
24. Jaramillo, F. & Hudspeth, A. J. (1993) *Neuron* **7,** 409–420.
25. Kroese, A. B. A., Das, A. & Hudspeth, A. J. (1989) *Hear. Res.* **37,** 203–218.
26. Howard, J. & Hudspeth, A. J. (1987) *Proc. Natl. Acad. Sci. USA* **84,** 3064–3068.
27. Herrmann, C., Wray, J., Travers, F. & Barman, T. (1992) *Biochemistry* **31,** 12227–12232.
28. Denk, W., Keolian, R. & Webb, W. W. (1992) *J. Neurophysiol.* **68,** 927–932.
29. Jaramillo, F. & Hudspeth, A. J. (1993) *Proc. Natl. Acad. Sci. USA* **90,** 1330–1334.
30. Howard, J. & Hudspeth, A. J. (1988) *Neuron* **1,** 189–199.
31. Russell, I. J., Kössl, M. & Richardson, G. P. (1992) *Proc. R. Soc. London Ser. B* **250,** 217–227.
32. Géléoc, G. S. G., Lennan, G. W. T., Richardson, G. P. & Kros, C. J. (1997) *Proc. R. Soc. London Ser. B* **264,** 611–621.
33. Wu, Y.-C., Ricci, A. J. & Fettiplace, R. (1999) *J. Neurophysiol.* **82,** 2171–2181.
34. Ricci, A. J., Crawford, A. C. & Fettiplace, R. (2002) *J. Neurosci.* **22,** 44–52.
35. Hudspeth, A. J. & Gillespie, P. G. (1994) *Neuron* **12,** 1–9.
36. Gillespie, P. G. & Corey, D. P. (1997) *Neuron* **19,** 955–958.
37. Eatock, R. A. (2000) *Annu. Rev. Neurosci.* **23,** 285–314.
38. Crawford, A. C. & Fettiplace, R. (1985) *J. Physiol. (London)* **364,** 359–379.
39. Ricci, A. J., Crawford, A. C. & Fettiplace, R. (2000) *J. Neurosci.* **20,** 7131–7142.
40. Assad, J. A., Hacohen, N. & Corey, D. P. (1989) *Proc. Natl. Acad. Sci. USA* **86,** 2918–2922.
41. Rüsch, A. & Thurm, U. (1990) *Hear. Res.* **48,** 247–264.
42. Assad, J. A. & Corey, D. P. (1992) *J. Neurosci.* **12,** 3291–3309.
43. Denk, W. & Webb, W. W. (1992) *Hear. Res.* **60,** 89–102.
44. Brix, J. & Manley, G. A. (1994) *Hear. Res.* **76,** 147–157.
45. Holt, J. R., Corey, D. P. & Eatock, R. A. (1997) *J. Neurosci.* **17,** 8739–8748.
46. Choe, Y., Magnasco, M. O. & Hudspeth, A. J. (1998) *Proc. Natl. Acad. Sci. USA* **95,** 15321–15326.
47. Markin, V. S. & Hudspeth, A. J. (1995) *Annu. Rev. Biophys. Biomol. Struct.* **24,** 59–83.
48. Jaramillo, F., Howard, J. & Hudspeth, A. J. (1990) in *The Mechanics and Biophysics of Hearing*, eds. Dallos, P., Geisler, C. D., Matthews, J. W., Ruggero, M. A. & Steele, C. R. (Springer, Berlin), pp. 26–33.
49. Crawford, A. C., Evans, M. G. & Fettiplace, R. (1991) *J. Physiol. (London)* **434,** 369–398.
50. Marquis, R. E. & Hudspeth, A. J. (1997) *Proc. Natl. Acad. Sci. USA* **94,** 11923–11928.
51. Eatock, R. A., Corey, D. P. & Hudspeth, A. J. (1987) *J. Neurosci.* **7,** 2821–2836.
52. Hacohen, N., Assad, J. A., Smith, W. J. & Corey, D. P. (1989) *J. Neurosci.* **9,** 3988–3997.
53. Walker, R. G. & Hudspeth, A. J. (1996) *Proc. Natl. Acad. Sci. USA* **93,** 2203–2207.
54. Cyr, J., Dumont, R. A. & Gillespie, P. G. (2002) *J. Neurosci.* **22,** 2487–2495.
55. Gillespie, P. G., Wagner, M. C. & Hudspeth, A. J. (1993) *Neuron* **11,** 581–594.
56. Holt, J. R., Gillespie, S. K. H., Provance, D. W., Jr., Shah, K., Shokat, K. M., Corey, D. P., Mercer, J. A. & Gillespie, P. G. (2002) *Cell* **108,** 371–381.
57. Howard, J. & Spudich, J. A. (1996) *Proc. Natl. Acad. Sci. USA* **93,** 4462–4464.

BIOPHYSICS